VACUUM SYSTEM DEVELOPMENT STATUS FOR THE APS STORAGE RING*

R. Wehrle, R. Nielsen, and S. Kim
Argonne National Laboratory
9700 S. Cass Avenue
Argonne, IL 60439-4814

Abstract

The status of the design and fabrication of a prototype sector of the storage ring vacuum system for the Advanced Photon Source is described. The 26.5-m-long prototype sector will be assembled within a full-scale magnet and tunnel mockup to study interspacial component relationships for maintenance, as well as the vacuum system operational performance. Each completed vacuum section is mounted as an integral part of the modular structure that contains the magnets and magnet power supplies on a common base. Unique automatic machine welding designs and techniques are employed in the fabrication of the aluminum vacuum chambers from extrusions. Special chamber bending procedures and measurement checks are used to maintain the required flatness of the inside chamber light gap surfaces. Photo-electron yields due to low-energy photons in the narrow channel gap of the vacuum chamber and their potential effects on the overall outgassing rate are found to be negligible.

Introduction

The Advanced Photon Source (APS) contains a positron storage ring for which the vacuum system is designed to maintain a beam-on pressure of 1 nTorr or less. This will enable attainment of beam lifetimes of approximately 20 hours.

Photo-electron yields due to low-energy photons in the narrow channel gap of the system vacuum chamber and their potential effects on the overall outgassing rate are discussed.

The vacuum chamber is constructed of 6063-T5 aluminum straight and bend extrusions with automatic machine weldments for positron, photon, pump and gauge ports. Nonevaporable getter (NeG) strips are the primary distributed vacuum pumping within both the straight and bend vacuum chamber sections. A prototype of a sector of the ring vacuum system, 1/40 of the ring circumference and approximately 26.5-m-long, is under construction. It will be used to study vacuum system performance and some aspects of maintenance. The prototype chamber is nearing completion. The status, design and fabrication and some results on the following items are described:

1. Vacuum chamber mounts,
2. NeG strip assemblies,
3. Main types of chamber weld,
4. Pump-down of a 30"-long welded test chamber, and
5. Auger tests of surface preparations of the chambers.

Photo-Electron Yield due to Low Energy Photons

The number of photo-electron yields, $\dot{N}_e$, may be calculated from

$$\dot{N}_e = \int_{\varepsilon_m} \frac{d\dot{N}}{d\varepsilon} Y(\varepsilon) d\varepsilon \ \text{(electrons/s)} \qquad (1)$$

where $\frac{d\dot{N}}{d\varepsilon}$ is the number of photons per eV of photon energy ε and the data by Mathewson et al. may be used for the photo-electron yield function $Y(\varepsilon)$ for Al oxide and Al[1,2]. The data indicate that the minimum photon energy ε_m for electron yield is ~10 eV.

The vertical angular spread of the photons for $\varepsilon << \varepsilon_c$ (photon critical energy) is given by[3]

$$2\Delta\psi(\text{FWHM}) = \frac{2}{\gamma}\left(\frac{\varepsilon_c}{\varepsilon}\right)^{1/3}. \qquad (2)$$

In the storage ring, the distance from radiation sources in the bending magnet to the chamber wall of the narrow beam channel area varies from 3.7 m to 17.5 m, which corresponds to the vertical angular spread $\Delta\psi$ = 1.4 - 0.3 mrad. From Eq. (3), the upper limits of energy ε of the photons that hit the wall are calculated to be 4.5 - 460 eV. Figure 1 shows the

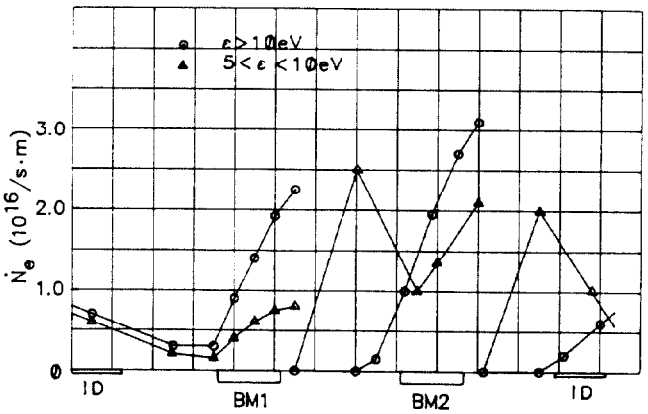

Fig. 1 Distribution of the photo-electrons over one sector of the APS storage ring

distribution of the photo-electron yield of Eq. (1) around the vacuum chamber of one sector of the storage-ring lattice. (Since the photo-electron yield below 10 eV is not known, the yield function $Y(\varepsilon)$ for $10 < \varepsilon < 73$ eV is used also for $5 < \varepsilon < 10$ eV.)

The photon-induced outgassing rate, when averaged over the photon energy, is given by[4]

$$\dot{Q} = \dot{N}\eta_{ph}\eta_e f(\phi), \qquad (3)$$

where η_{ph} is the average photo-electron yield per photon and η_e the molecular yield per photo-electron. The function $f(\phi)$ depends on the glancing angle ϕ of the photon beam to the vacuum-chamber wall. For ϕ less than 10 mrad, $f(\phi)$ approaches ~ 10. Since the coefficient η_e in Eq. (3) is not known, an empirical relation[5]

$$\dot{Q} = 2\dot{N}(n\gamma)K \qquad (4)$$

is often used for the calculation of the photon-induced outgassing. Here, $n\gamma$ is dosage-dependent molecular yield per photon (2×10^{-7} mol/photon after 150 A·h of bombardment, for example) and K is a constant 3.11×10^{-20} Torr ℓ/mol.

The total number of $\dot{N}_e$ from the surface of the narrow channel around the storage ring is

*Work supported by U.S. Department of Energy, Office of Basic Energy Sciences, under Contract No. W-31-109-ENG-38

0.8×10^{19} electrons/s for $\varepsilon > 10$ eV photons. (Approximately the same number of electrons is calculated for $5 < \varepsilon < 10$ eV photons.) When averaged around the storage ring, the upper limit of the average photon energy is only about 18 eV. The above photo-electron yield is approximately 17% of the total of photo-electron yield in the storage ring. (Only 2% of the total number of photons is responsible for the above photo-electrons.) The thermal energy deposition at the narrow-channel surface is calculated as less than 1 mW/cm^2.

Without knowing η_e in Eq. (3), the effects of the overall photon-induced outgassing rate in the vacuum chamber, due to the photo-electrons from the narrow channel, are discussed. Since the low-energy photons hit the edge of the narrow chamber wall near the antechamber with a glancing angle of 1 mrad, any outgassing related to the photo-electrons would diffuse directly into the antechamber. This would not change the average coefficient in Eq. (4).

There are experimental data on the storage-ring energy dependence of the pressure rise by Grobner et al.[6] The data show that below 0.8 GeV, which corresponds to the photon critical energy of 300 eV in their experiment, photon beams with glancing angle of 11 mrad do not contribute to the total specific pressure rise at all. The paper suggests that, as the glancing angle of the photon beam is decreased, the interaction of the photons occurs closer to the surface, and consequently the desorption by the photons of higher energy becomes more and more important. This suggests that the photons with energies less than 460 eV (average upper limit of 18 eV) and glancing angle less than 1.4 mrad would not contribute to the outgassing rate in the chamber.

The total number of photons and the pressure rise in a given storage ring should be proportional to the ring energy. The data by Halama[4] show that, at higher ring energy, there is an additional rise in pressure due to higher critical energy of the photon beam. This seems to be consistent with the implications of the data by Grobner et al.[6]

The above discussions indicate that the low-energy photons that hit the narrow channel wall would not affect the estimation of the outgassing rate as per Eq. (5) in the vacuum chamber of the APS storage ring.

Vacuum Chamber Mounts

The mounting of a typical straight section is shown in Fig. 2. Three mounts are used per straight section. One mount is rigid and does not allow chamber motion at the point of support in any direction. Its position is usually located approximately in the center of the section as shown. The other two mounts are each located at the ends of the chamber. These two mounts are essentially leaf springs allowing for the slight chamber thermal expansion along the beam line direction occurring during the vacuum bake cycle.

The mounting of a bend section is also accomplished with three mounts, as shown in Fig. 3. It has the two leaf spring mounts located at the ends of the chamber to allow thermal expansion in the approximate beam direction. The center mount of the bend section, unlike the rigid mount of the straight section, allows for the motion in the direction of increasing bend radius that occurs during the bake cycle. The midpoint of the bend section is maintained in a level position and is also constrained in the

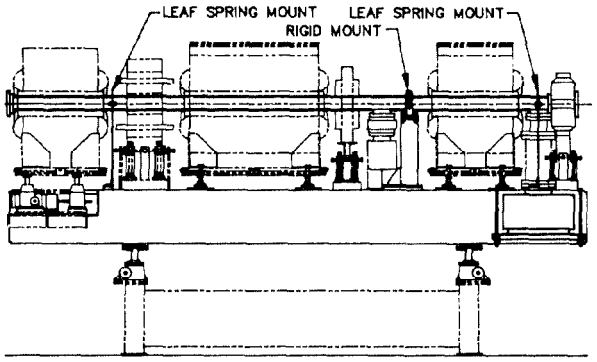

Fig. 2 Straight Section Mounting

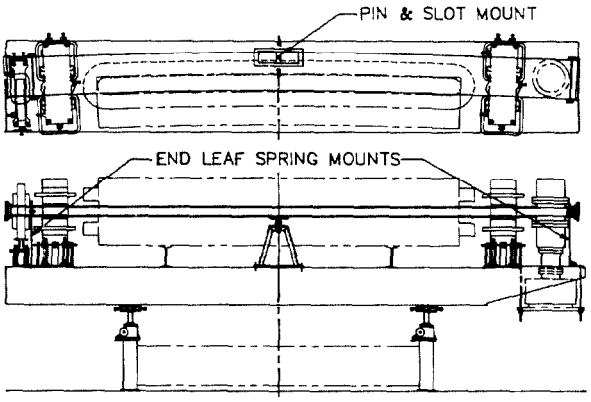

Fig. 3 Magnet Bend Section Mounting

beam direction. However, the section midpoint is allowed to move radially inward in the direction of its natural radial expansion by means of a pin and slot guide.

The salient aspect of both these chamber support mount systems is that the chambers are free to thermally expand with negligible forces placed on them. These mounting systems ensure that the chambers are not distorted in any manner and that they return to their original location, size, shape and geometry after each bake cycle.

NeG Strip Mount Assemblies

The operation of the NeG strips in the APS positron storage ring as the primary source of distributed pumping to obtain beam-on pressure of 1 nTorr or less has been previously described[7]. Some details of the NeG strip mounting assemblies are shown in Fig. 4. The stainless steel base mount strip is contained in the top and bottom antechamber walls within grooved tracks. The NeG strip is supported by stainless steel clips, which are attached to but electrically isolated from the base strip by ceramic insulators. This mode of mounting the NeG strips is similar to that used in LEP. However, the NeG assemblies in the APS are designed to be replaceable.

For replacement, the NeG assemblies in Fig. 5 can be removed from or inserted into one end of each vacuum chamber through a conflat vacuum seal opening. The conflat contains two miniature conflat seals, each with an electrical feed-through terminal. Sliding multiple contact band receptacles connect the terminals to the top and bottom NeG strips. The top and bottom NeG strips are connected together at the opposite end of the vacuum extrusion by a copper clip. This assembly system assures that the electrical connections remain stationary at the conflat end

insertion points while allowing the clip connection end to move freely during activation periods of the NeG strips, thus compensating for thermal expansion and contraction of the base strip.

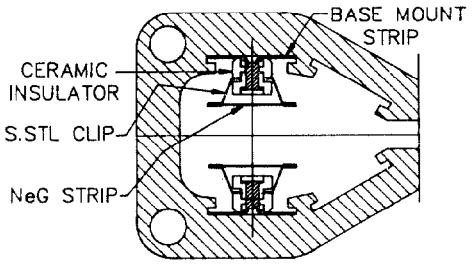

Fig. 4 End View of NeG Strip Mounting

Vacuum Chamber Weldments

The end flanges of the vacuum chamber are joined to the ends of the vacuum chamber extrusions with full penetration weldments. The inside surface of the weld bead is even with the beam chamber inside surface for low rf impedance. The ends of the sector terminate in an elliptical tube beam chamber, which also has a full penetration weldment with a similar inside surface. The photon exit block port is a full penetration weldment to the side of the chamber. The conflat weldments are inside vacuum welds, either of a filet or butt type. The large, 12"-diameter crotch absorber conflat weld follows the contour of the extrusion shape. These exacting weldments are done by an automated computer-controlled welding machine. They can be duplicated with high integrity.

A 30"-long sample of the extruded chamber has been manufactured (weld joints machined, chemically cleaned, end flanges and pump port welded in place) and vacuum tested. Helium leak testing to a sensitivity of 2×10^{-10} std. cm^3 helium/s indicated no leaks to the atmosphere. The system was roughed out using a turbomolecular pump and then baked at 150° C for 24 hours. As the chamber cooled after the bake cycle, pumping was transferred from the turbo pump to a 220 ℓ/sec ion pump which produced chamber pressure of 0.1 n Torr within 17 hours. The chamber has remained at that pressure, indicating no virtual leaks. The outgassing rate was calculated to be 3.2×10^{-12} Torr$\cdot\ell/cm^2\cdot$s.

The aluminum vacuum chambers will be chemically processed to provide a clean vacuum surface. Alkaline degreasers and etchants have been tested, and Auger analysis of the cleaned surfaces has indicated comparable results with those of Mathewson at LEP.[8,9] Since the 6063 alloy is magnesium based, the extruded surface consists of a magnesium oxide layer, which contains most of the surface contamination. The first cleaning step consists of a degreasing agent as well as an agent to remove the magnesium oxide layer. Once the magnesium oxide is removed, the second step uses an etchant (sodium hydroxide or potassium hydroxide based) to reduce the aluminum oxide layer. A final water rinse and blow drying completes the cleaning procedure.

The inside surface flatness of the bend chamber gaps was checked with survey equipment. A small steel target disk was moved to coordinate positions with an outside magnet on both bottom and top surfaces and sighted. The best two of the first six chambers bent had surfaces within a millimeter flatness. This should be improved by fixture adjustments for the next six test bends as development work proceeds.

References

1. A.G. Mathewson, G. Horikoshi, and H. Mizuno, "Some Notes on the Photoelectron Induced Gas Desorption Problems in the Photon Factory and Tristan," KEK-78-9 (1978).

2. ESRF Vacuum Workshop Report (1987).

3. R.A. Mack, "Spectral and Angular Distribution of Synchrotron Radiation," CEAL-1027 (1966).

4. H.J. Halama, "Electron Storage Ring Beam Lifetime Dependence on Pressure and Pumping Speed," J. Vac. Sci. Tech. A3, 1699 (1985).

5. S. Tazzari, "Synchrotron Radiation Distribution along the Vacuum Chamber," European Synchrotron Radiation Project Report, ESRP-IRM-32/84 (1984).

6. O. Gröbner, A.G. Mathewson, H. Stori, and P. Stubin, "Studies of Photon Induced Gas Desorption using Synchrotron Radiation, Vacuum," 33, 397-406 (1983).

7. R. Wehrle, J. Moenich, S. Kim, and R. Nielsen, "Vacuum System for the Synchrotron X-Ray Source at Argonne," IEEE Particle Accelerator Conf., Vol. 3 (1987).

8. A.G. Mathewson, "The Temperature and Time Dependence of the Cleaning Efficiency of the Alkaline Detergent Almeco 18," LEP Vacuum Technical Note (January 15, 1986).

9. A.G. Mathewson, "The Effect of Amklene on the Surface Composition of Extruded Al Alloy at Different Temperatures," LEP Vacuum Technical Note (1986).

Acknowledgements

The authors are grateful for the challenging weld developments of W. Farrell and group at Ferranti Sciaky, Inc.; the chamber bends by R. Shiamias of Pacific Pipe Co.; and the excellent contributions of E. Wallace, R. Swanstrom, R. Benaroya, and the expertise of Mansoo Choi to the APS vacuum system.

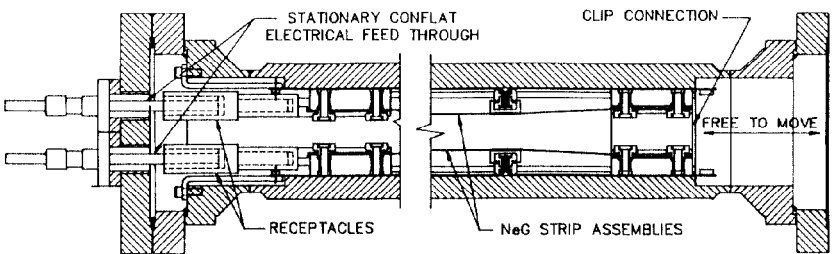

Fig. 5 NeG Assemblies